A Nested Grid Computation for the Barotropic Free Surface Atmosphere

Jiun H. Chen[1] and Kikuro Miyakoda

Geophysical Fluid Dynamics Laboratory/NOAA, Princeton University, Princeton, N. J. 08540

(Manuscript received 25 September 1973, in revised form 8 January 1974)

ABSTRACT

The nested grid is used in a barotropic free surface model. Two grids are nested; one is a coarse mesh grid that covers a large region and the other a fine mesh grid set in a limited area inside the larger region. The interaction between the two grids is one-directional; the boundary condition for the smaller domain is taken from the solutions of the larger domain. The two major problems are how to select appropriate boundary settings for the limited area fine mesh grid and to evaluate how quickly the boundary error grows and invades the inner domain. Two methods of boundary setting are proposed; one is to specify a set of well-posed "physical" boundary conditions as well as to provide the "computational" boundary conditions by using "upwind" extrapolation and "pseudo-characteristic" extrapolation methods. The other is to specify all variables at all boundaries as they are taken from the solutions of the larger area coarse mesh grid and to apply "boundary smoothing" in order to suppress the computational modes. Tests indicate that the solutions for the nested fine mesh appear satisfactory with both methods up to 6.5 days. The semi-implicit difference scheme proves to be particularly efficient for the nested grid calculation.

1. Introduction

The numerical simulation of the medium- (1000–100 km) and meso-scale (100–10 km) phenomena of the atmosphere such as frontal waves, hurricanes, cloud clusters, squall lines, and frontal zones requires a grid with a very small mesh size, say 5 km to 50 km. Because of the limitation of the computing capacity, it is extremely difficult, if not impossible, to fill the entire globe or even one hemisphere homogeneously with such a fine mesh. A reasonable way to handle this type of problem is perhaps to apply a limited area model with a fine grid resolution to the region of concern. However, the omission of the effect of the evolution outside the limited domain distorts the overall solution inside the domain rather quicikly.

In order to overcome or at least alleviate this difficulty a "nested grid" or "nested mesh" system is being considered, and in fact, simple versions of the model have already been worked out by several people. The system consists of a limited fine mesh area embedded within a larger domain of coarse mesh. Multiple meshes are sometimes used stepwise so as to reduce the grid size less suddenly and are called the "telescopic mesh."

One of the most crucial problems in the nesting of meshes is how to connect the solutions from the various meshes. In general, two approaches have been proposed. The first approach allows full interaction of the solutions between meshes (Birchfield, 1960; Matsuno, 1966; Koss, 1971; Harrison and Elsberry, 1972; Mathur, 1972; Ookochi, 1972; Jones, 1973; Price and MacPher-

son, 1973; and Phillips and Shukla, 1973). In this system, the exchanges of momentum and energy between meshes are thoroughly considered. It is interesting to note, however, that most of the successful models in this category (except that of Price and MacPherson, 1973) are related to the hurricane problem, whose environmental domain has a rather uniform and calm flow field. Matsuno (1966) and Browning et al. (1973) found that wave motions in two unequal meshes have different phase speeds due to the truncation error, and, as a consequence, numerical trouble usually develops.

The other approach allows effect in only one direction, that is from the outer mesh to the inner mesh, and not vice versa. In other words, the solution for the entire domain is calculated with the coarse mesh grid, and then the solution thus obtained is used to specify the boundary conditions of the limited domain for the fine mesh grid, where the specified boundary conditions vary with time. Let us call it the "one-directional nested grid method" (Howcroft, 1966; Hill, 1968; Wang and Halpern, 1970; Shapiro and O'Brien, 1970; Bengtsson and Moen, 1971; Asselin, 1972; Williamson, 1973; Elvius and Sundström, 1973; and Davies, 1973). In this system, not only the larger scale motion such as planetary scale waves but also the synoptic scale motion such as cyclone or anticyclone systems which move outside the domain must be taken care of through the temporally varying boundary conditions. The local atmospheric phenomena that are produced by the fine-structured topography, the land-sea contrast, the low-level jet, the moisture tongue, or the ensembled cumulus convection are treated inside the small domain. There

is a disadvantage with this approach, i.e., circulations that may be developed or enhanced by changes in the LFM and whose effects may reach the CM outside cannot be handled by using this approach. Therefore, in such a situation, a larger LFM area may be needed so that the boundary stays out of the region where these effects are strong.

Thus each approach has merit as well as demerit. If, for example, one is interested in the solution in the whole domain, the first approach is the only way. But, if one is concerned only with the fine scale solution inside the small domain, both the first and the second approaches are usable. However, the second approach appears advantageous from the standpoint of being able to obtain a stable numerical solution easily. Furthermore, the latter approach requires less computer storage than the first approach, where the coarse mesh and the limited-area fine mesh calculations have to be carried out simultaneously. It is the second approach that we shall adopt here. In the present study, our concern is to develop the nested grid technique itself, so we shall use a simple atmospheric model—a barotropic free surface model—and the two mesh system, where the ratio of grid sizes is 2 to 1 in this particular case.

We shall use explicit schemes of both leap-frog and Euler-backward methods and a semi-implicit scheme. Both leap-frog, explicit and semi-implicit schemes are faster in speed than the Euler-backward explicit scheme and are therefore attractive. The Euler-backward explicit scheme, however, is capable of handling noise and is therefore expected to be useful for the nested grid problem for which some noise from the mesh interface is unavoidable.

2. Governing equations

The equations for a two-dimensional free surface model are written as,

$$\frac{\partial}{\partial t}u + m\left(u\frac{\partial}{\partial x}u + v\frac{\partial}{\partial y}u\right) = \hat{f}v - m\frac{\partial}{\partial x}\Phi, \quad (1A)$$

$$\frac{\partial}{\partial t}v + m\left(u\frac{\partial}{\partial x}v + v\frac{\partial}{\partial y}v\right) = -\hat{f}u - m\frac{\partial}{\partial y}\Phi, \quad (1B)$$

$$\frac{\partial}{\partial t}\Phi + m^2\left[\frac{\partial}{\partial x}\left(\Phi\frac{u}{m}\right) + \frac{\partial}{\partial y}\left(\Phi\frac{v}{m}\right)\right] = 0 \quad (1C)$$

where u and v are the velocity components in x and y directions, Φ is the geopotential height, m is the map scale factor, i.e., $m = 2/(1+\sin\theta)$, where θ is the latitude, and $\hat{f}$ is defined as follows:

$$\hat{f} = f + m^2\left(v\frac{\partial}{\partial x}\frac{1}{m} - u\frac{\partial}{\partial y}\frac{1}{m}\right),$$

where f is the Coriolis parameter.

To solve this set of equations, the equations are first approximated by finite difference equations, using the grid system shown in Fig. 1, where Δ is the mesh size. The variables are specified in the "staggered" grid; i.e., u, v, and ϕ are defined at different locations (Williams, 1969). This kind of grid (i.e., a staggered grid) system seems rather convenient, if not necessary, in order to apply the "semi-implicit scheme" which will be described later.

Let us first define the following basic finite difference operators, i.e.,

$$\overline{Q}^x = \tfrac{1}{2}(Q_{i+\frac{1}{2}} + Q_{i-\frac{1}{2}}),$$

$$Q_x = (Q_{i+\frac{1}{2}} - Q_{i-\frac{1}{2}}),$$

$$\langle Q \rangle = \tfrac{1}{2}[Q(t+\Delta t) + Q(t-\Delta t)],$$

$$\overline{Q}^{2x} = \tfrac{1}{2}(Q_{i+1} + Q_{i-1}),$$

and their compound operators,

$$\overline{Q}^{xy} = (\overline{\overline{Q}^x})^y,$$

$$Q_{xx} = (Q_x)_x, \text{ etc.}$$

where Q is an arbitrary variable, i is the index of the grid in x coordinate and Δt is the time increment.

In what follows, we will use two schemes for numerical time integration; one is the "explicit" scheme and the other is the "semi-implicit" scheme, where the latter is employed for the purpose of speeding up the calculation.

a. The explicit scheme

The Eqs. (1A), (1B), and (1C) are approximated by finite difference equations as
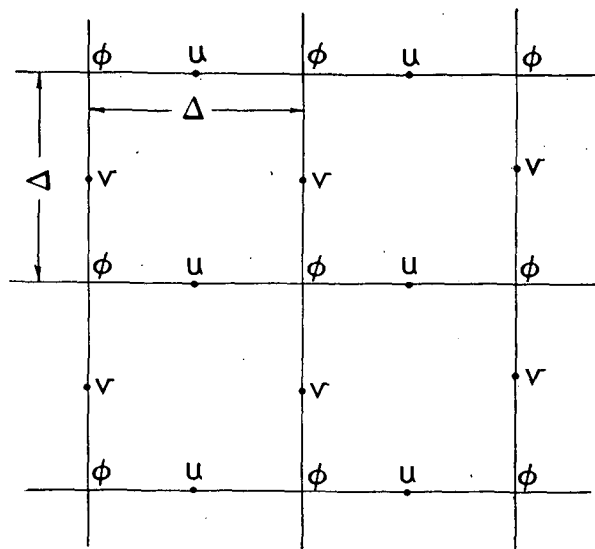

FIG. 1. Locations of u, v, and ϕ on the staggered grid.

$$u(t+\Delta t)-u(t-\Delta t)$$

$$=-C(V,u)+2\Delta t\overline{fv}^{-xy}-2\frac{\Delta t}{\Delta}^{-x}m\,\phi_x, \quad (2A)$$

$$v(t+\Delta t)-v(t-\Delta t)$$

$$=-C(V,v)-2\Delta t\overline{fu}^{-xy}-2\frac{\Delta t}{\Delta}^{-y}m\,\phi_y \quad (2B)$$

$$\phi(t+\Delta t)-\phi(t-\Delta t)=-2\frac{\Delta t}{\Delta}\Phi_0 m^2[(u/\overline{m}^{\,x})_x+(v/\overline{m}^{\,y})_y]$$

$$-2\frac{\Delta t}{\Delta}m^2[(\overline{u\phi}^{\,x}/\overline{m}^{\,x})_x+(\overline{v\phi}^{\,y}/\overline{m}^{\,y})_y] \quad (2C)$$

where Φ is divided into two, for future purposes, i.e., Φ_0, the mean geopotential height which is constant with space and time, and $\phi=\Phi-\Phi_0$, the deviation from the mean height. The nonlinear term is treated the same way as in the generalized Arakawa scheme, which was proposed by Grammeltvedt[2] (1969). The scheme is further modified to include the map scale factor m. Thus the term C is written as

$$C(V,u)=\frac{2}{3}\frac{\Delta t}{\Delta}\overline{m}^{\,x}[\{2\overline{uu_x}^{\,x}+\overline{u}^{\,2x}\overline{u_x}^{\,x}\}$$

$$+\tfrac{1}{2}\{\overline{u_{xx}u_x}^{\,x}+(\overline{u\nabla^2 u})_x^{\,x}\}/(\overline{m}^{\,x})^2$$

$$+3\overline{v}^{\,xy}\overline{u_y}^{\,y}+\tfrac{1}{4}\{\overline{v_y u_{yy}}^{\,x}\}/(\overline{m}^{\,x})^2],$$

and

$$C(V,v)=\frac{2}{3}\frac{\Delta t}{\Delta}\overline{m}^{\,y}[2\overline{vv_y}^{\,y}+\overline{v}^{\,2y}\overline{v_y}^{\,y}$$

$$+\tfrac{1}{2}\{\overline{v_{yy}v_y}^{\,y}+(\overline{v\nabla^2 v})_y^{\,y}\}/(\overline{m}^{\,y})^2$$

$$+3\overline{u}^{\,xy}\overline{v_x}^{\,x}+\tfrac{1}{4}\{\overline{u_x v_{xx}}^{\,y}\}/(\overline{m}^{\,y})^2],$$

where ∇^2 is a discrete Laplacian, i.e., $\nabla^2 Q=Q_{xx}+Q_{yy}$.

As seen in these expressions, the spatial differencing is fourth order for u in x and v in y, whereas the original differential equations are first order. This means that four boundary conditions are required for both u in x and v in y, one of which is "physical" and the other three are "computational" boundary conditions. To provide some of the computational boundary conditions, a second order difference equation based on central difference is used next to the x (or y) boundaries for u (or v) equation. Thus each provides two conditions.

---

[2] Grammeltvedt (1969) asserted that this scheme guarantees not only the kinetic energy conservation but also the enstrophy conservation for the non-divergent component of flow. It appears that the enstrophy conservation is not exact, but this scheme seems to provide a fairly stable calculation, though it is somewhat complicated.

The other computational as well as the physical boundary conditions will be discussed in Section 4.

Although in Eqs. (2A), (2B), and (2C), the "leap-frog" method is shown for time differencing, we have also employed the "Euler-backward" method (Matsuno, 1966; Kurihara, 1965). If we represent the former by

$$u(t+\Delta t)-u(t-\Delta t)=F(t),$$

then the latter would be written as

$$u^*-u(t)=\tfrac{1}{2}F(t),$$

$$u(t+\Delta t)-u(t)=\tfrac{1}{2}F^*$$

where F^* is calculated from the intermediate solutions for u^*, v^*, and ϕ^*.

b. The semi-implicit scheme

The semi-implicit scheme, written by Renfrew (1971), is based on the method of Robert (1969) (see also Kwizak and Robert, 1971; and McPherson, 1971), in which the implicit treatment is applied only to the gravity wave components, not to the nonlinear terms. The semi-implicit scheme avoids the complications of iteration characteristic of a fully implicit scheme. According to this scheme, the implicit treatment is applied to the terms of the spatial gradient of geopotential height in the equations of motion and to the term of the two-dimensional flow divergence that is multiplied by the mean geopotential height in the continuity equation. Specifically, in Eqs. (2A), (2B), and (2C), we make the following modifications, i.e.,

$$2\phi_x(t)\to\phi_x(t+\Delta t)+\phi_x(t-\Delta t),$$

$$2\phi_y(t)\to\phi_y(t+\Delta t)+\phi_y(t-\Delta t),$$

and

$$2\Phi_0[(u/\overline{m}^{\,x})_x+(v/\overline{m}^{\,y})_y]$$

$$\to\Phi_0[(u(t+\Delta t)+u(t-\Delta t)/\overline{m}^{\,x})_x$$

$$+(v(t+\Delta t)+v(t-\Delta t)/\overline{m}^{\,y})_y].$$

Inserting these expression into (2A), (2B), and (2C), using the central difference for the time derivatives, and manipulating the resulting equations, one derives

$$\langle u\rangle+\frac{\Delta t}{\Delta}\overline{m}^{\,x}\langle\phi_x\rangle=r_1. \quad (3A)$$

$$\langle v\rangle+\frac{\Delta t}{\Delta}\overline{m}^{\,y}\langle\phi_y\rangle=r_2, \quad (3B)$$

$$\langle\phi\rangle+\frac{\Delta t}{\Delta}m^2\Phi_0[(\langle u\rangle/\overline{m}^{\,x})_x+(\langle v\rangle/\overline{m}^{\,y})_y]=r_3, \quad (3C)$$
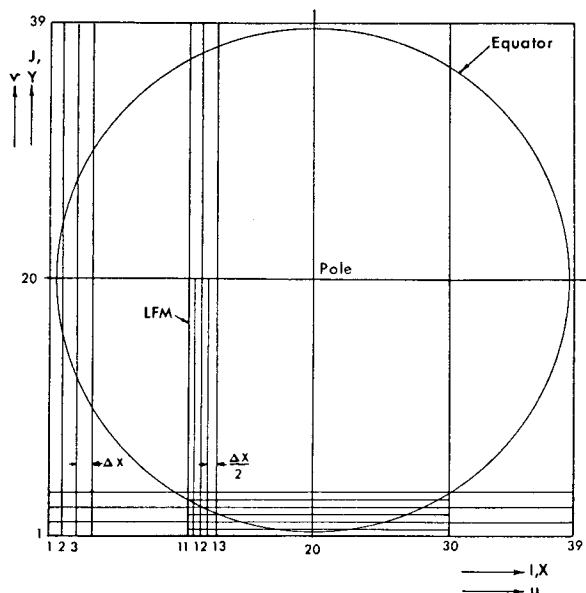
FIG. 2. Large area coarse mesh and limited-area fine mesh (LFM), which is located in the lower middle part of the large area, i.e., I from 11 to 30 and J from 1 to 20.

where

$$r_1 \equiv -\tfrac{1}{2}C(\mathbf{V},u)+\Delta t \overline{fv}^{-xy}+u(t-\Delta t),$$

$$r_2 \equiv -\tfrac{1}{2}C(\mathbf{V},v)-\Delta t \overline{fu}^{-xy}+v(t-\Delta t),$$

$$r_3 \equiv -\frac{\Delta t}{\Delta}m^2[(\overline{u\phi}^{-x}/\overline{m}^{-x})_x+(\overline{v\phi}^{-y}/\overline{m}^{-y})_y]+\phi(t-\Delta t),$$

and C is the same as in the explicit scheme. In Eqs. (3A), (3B), and (3C), the unknown variables are $\langle u \rangle$, $\langle v \rangle$, and $\langle \phi \rangle$. In order to solve this set of simultaneous equations, we eliminate $\langle u \rangle$ and $\langle v \rangle$ from these equation in favor of $\langle \phi \rangle$ and obtain,

$$\langle \phi \rangle - \left[\frac{\Delta t}{\Delta}\right]^2 m^2\Phi_0[\langle \phi \rangle_{xx}+\langle \phi \rangle_{yy}]=r_4 \ . \tag{4}$$

where

$$r_4=r_3-\frac{\Delta t}{\Delta}m^2\Phi_0[(r_1/\overline{m}^{-x})_x+(r_2/\overline{m_y}^{-y})_y].$$

This is a Helmholtz equation in $\langle \phi \rangle$, and r_4 is the forcing function, which is known at the time t.

To solve the Helmholtz equation numerically, a number of methods are available. The DRM (the Dimension Reduction Method) (Ogura and Charney, 1961; Hockney, 1965; Ogura, 1969) is the most superior in speed on a rectangular grid system but is not usable for an irregular domain. The ADI method (Alternating Direction Implicit) (Peaceman and Rachford, 1955; Birkhoff et al., 1962) is very fast and relatively easy to handle even for an irregular domain. The SOR method

(Successive Over-Relaxation) (see Fox, 1962, for example) is the simplest in treatment and is relatively fast. According to our experience, ADI is roughly 2 to 3 times faster than SOR for the two-dimensional 20 × 20 grid and this ratio increases as the grid dimensions increase (Miyakoda, 1960). Due to the above consideration, we use the ADI method in our calculation.

After solving for $\langle \phi \rangle$, the final results for the three variables are obtained from

$$u(t+\Delta t)=-2\frac{\Delta t}{\Delta}\overline{m}^{-x}\langle \phi_x \rangle+2r_1-u(t-\Delta t), \tag{5A}$$

$$v(t+\Delta t)=-2\frac{\Delta t}{\Delta}\overline{m}^{-y}\langle \phi_y \rangle+2r_2-v(t-\Delta t), \tag{5B}$$

$$\phi(t+\Delta t)=2\langle \phi \rangle-\phi(t-\Delta t). \tag{5C}$$

3. Mesh system

The system of nested grids used here consists of two grids. In both grids, the Cartesian coordinates on a stereographic projection map are used. The large area is a square (for simplicity) which covers one entire hemisphere and parts of the other hemisphere which are included in the four corner regions. Two grid resolutions, a coarse mesh and a fine mesh, are used for the large domain, so that we have a large domain coarse mesh (CM), and a large domain fine mesh (FM). For the large domain coarse mesh, $\nu=39$ is used, whereas for the large domain fine mesh, $\nu=77$ is used, where ν is the dimension of the square array of equal grid size Δ on the projection map. The grid sizes for these two meshes are in the ratio of 2 to 1 and correspond to about 540 km and 270 km in the middle latitude. The total number of gripdoints in the $\nu=39$ grid, for example, are 39×39, 40×39, and 39×40 for the fields of the geopotential height, ϕ, and the velocity components, u and v, respectively.

For the limited area, the same fine mesh but $\nu=39$ dimension is used, which is referred to as the limited-area fine mesh (LFM). The size of the limited area is one quarter of the large domain, and the location is chosen in the lower middle part of the large domain (Fig. 2). Therefore, the south boundary of the small domain coincides with a boundary of the large domain. The other boundaries of this small domain are located in regions of active disturbances, so it is expected that a critical and fair test can be made for this nesting of meshes. The dynamical models for the limited domain are identical to those for the larger domain in regards to the total number of gridpoints and physics.

4. Boundary conditions

We have to consider two types of boundary settings, i.e., one for the large domain and the other for the small domain. The larger domain has the usual boundary conditions, whereas boundary conditions of the small

domain are special and are our main concern in this paper.

Concerning the large domain, we assumed that it is closed for the momentum flux and the boundary has a no-shear slip condition. The small domain is, on the other hand, open and fluxes are allowed to pass through the border lines. Boundary conditions for a limited domain were discussed previously by Charney (1962). He concluded that an appropriate set of boundary conditions for the balanced barotropic equations is to specify the normal velocity component at all boundaries and the potential vorticity at inflow boundaries, and that this set of conditions is necessary and sufficient. Asselin (1972), on the other hand, used a slightly different set of boundary conditions: the normal velocity component is specified at all boundaries and the absolute vorticity at inflow boundaries. He applied these conditions for the nested grid calculation, and obtained successfully stable solutions for the small domain.

We here propose a new set of boundary conditions:[3] *the normal velocity component is specified at all boundaries and the tangential component at the inflow boundaries.* This set of conditions is supposed to be applied to differential equations. There is, however, a problem when it is applied to difference equations. As Chen (1971) discussed previously, it is often the case that the order of spatial difference in a difference equation is increased compared with the order of derivative in the original differential equations, and in this case the system of equations requires not only "physical" boundary conditions but also "computational" boundary conditions. The latter conditions or *the extraneous conditions should normally be provided by the governing equations or equations derived from them.* In other words, the computational boundary values should be obtained by extrapolation from the solution inside with the governing equations.

In order to extrapolate the values at the incoming as well as the outgoing boundaries, the theory of characteristics can be utilized. For the one-dimensional case, Chen (1973) showed how to apply the "characteristic extrapolation." In a two-dimensional case, three-dimensional (including the time coordinate) characteristics, called the "Monge cones," (see, for example, Garabedian, 1964) are obtained. A Monge cone consists of a family of characteristic generators which travel in different directions, so it cannot be used to write a one-sided difference equation for the purpose of boundary value extrapolations. For this reason "pseudo-characteristics," derived in the Appendix, are used. Thus a set of well-posed boundary conditions will be formulated as in the following. The newly proposed set of physical boundary conditions, which was described in the previous paragraph, is used as the base, and the computational boundary conditions are

obtained by extrapolation using the "pseudo-characteristic" or the advection equation. This set of boundary conditions provides one of the nesting methods which will be referred to as Set (5) later.

The following method proposed by Chen (1973) will be referred to as Set (4). In order to explain this method, let us consider the following set of boundary conditions: all variables are taken from the solutions of the larger domain and are specified at all boundaries of the smaller domain. It is known that this set of boundary conditions is overspecified. However, our case is special; the values from the large domain solutions are supposedly very close to satisfying the difference equations of the smaller domain, if the physics included in both models are the same. In other words, the boundary values in the set mentioned above are *almost* compatible among themselves under the limited domain model. Chen (1973) asserted that in this special case the over-specification may be allowed to a certain extent, when "boundary smoothing" is used.[4] The boundary smoothing is applied only to the grid points next to the boundary. The function of local boundary smoothing is to link together different modes of computational solutions, so that computational modes are suppressed whereas the physical modes are not much modified. The merit of this boundary setting is that it does not depend on the particular kind of governing equations, i.e., no knowledge of any set of well-posed boundary conditions is needed. It is applicable to either hyperbolic or elliptic type equations.

Let us next explain the other sets of boundary conditions which will be tested. The first two sets mentioned below, i.e., Set (1) and Set (2), (they were also studied by both Platzman, 1954, and Nitta, 1962, for the one-dimensional advection equation) are not suitable for nested grids, but they are used here for comparison. Any useful nested grid should give better solutions than those obtained with these sets of boundary conditions. Set (3) is the Dirichlet condition, where the solutions from the large area coarse mesh grid are specified at the boundaries of the limited area. This is the simplest method and is, therefore, attractive, but as was mentioned earlier, the set is an over-specification.

Set (1): Fixed boundary values
  All variables, u, v and ϕ, at all boundaries are kept constant for all time.

Set (2): The Neumann condition
  Derivatives normal to the boundaries for all variables u, v and ϕ are set equal to zero at all boundaries. For example, at the west boundary, it is specified that $u_{1,j} = u_{2,j}$ where 1 and 2 are the grid index for the x direction and j is the grid index for the y direction.

---

[3] While we were preparing the final draft of this manuscript, a paper by Elvius and Sundström (1973) just came out in which they also used the same (physical) boundary conditions.

[4] A number of people have proposed something similar. They use smoothing over several grid layers instead of only one in our case next to the boundary. The main difference between their methods and ours is that theirs is a theoretical justification for our method.
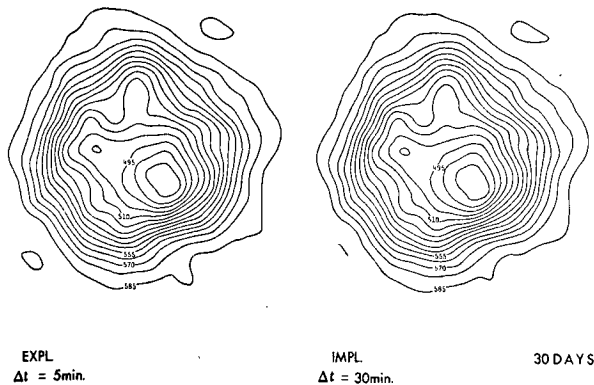
EXPL　　　　　　　　　　　IMPL.　　　　　　　30 DAYS
Δt = 5min.　　　　　　　　Δt = 30min.

FIG. 3. Height contour lines at day 30 with the Explicit Scheme (EXPL) and the Semi-Implicit Scheme (IMPL). The unit of contours is 10 m.

Set (3): The Dirichlet condition

All variables, u, v and ϕ, are provided by the solutions from the large area coarse mesh grid at all boundary points, therefore, the boundary values vary with time as the large area solutions evolve. Linear interpolations in time and space are used whenever necessary. This is an overspecification.

Set (4):The Dirichlet conditions with local boundary smoothing

In addition to the Dirichlet conditions specified in Set (3), local boundary smoothing is applied to all variables at the gridpoints next to the boundaries. For example, the smoothing algorithm for u at the west boundary is

$$u_{2,j}(\text{smoothed}) = \tfrac{1}{2}u_{2,j} + \tfrac{1}{4}(u_{1,j} + u_{3,j}).$$

Note that the smoothing is applied in the direction normal to the boundary inside the small domain.

Set (5): Well-posed conditions

The normal velocity component at all boundary points and the tangential component at the inflow boundary points are specified. In addition, the tangential velocity component at the outflow boundary points is extrapolated by the "upwind method" using (1A) or (1B) (see Chen, 1973), and the geopotential height ϕ at boundary points everywhere is extrapolated by the "pseudo-characteristic method" using (P1) or (P2) in the Appendix.

Sets (4) and (5) are the sets of conditions that we think best. Our opinion is based on the earlier discussion and also on our experimental results as described later.

5. Tests

It is noted that in the Euler-backward method, in which the advance to a new time level involves two

steps, the boundary values must be set at both steps. Further, Chen (1971) found that the values for the two steps must be identical in order to suppress the computational modes created by the use of a two-step scheme. Therefore, the boundary conditions of the first step are specified as described above in this section and the boundary values of the second step at the same time level are assigned the same values as in the first step.

For the explicit scheme, a CM calculation is first carried out, LFM calculations using boundary conditions Set (1) to Set (5) are then performed. For the semi-implicit scheme, a CM calculation is carried out, then a LFM calculation using Set (4)[5] is performed. When the grid discrepancy is introduced, error starts to grow at the boundary and propagates towards the interior. It is our objective to test the boundary conditions to see whether reasonable solutions can be obtained for a certain length of time, and also to see how quickly the error propagates inside the small domain.

In order to evaluate quantitatively the amount of error in the nested grid solution, we compute a "reference solution" by carrying out the FM calculation of the explicit scheme. The solutions obtained in the nested grid calculations of the explicit scheme are compared with this reference solution. (No FM calculation of the semi-implicit scheme is done because of the computer storage limitation.) Real data for the 500-mb geopotential height treated with an initialization routine was employed as the initial condition. The initial condition for LFM uses the same value in the limited area. That for CM uses the same value at points common to both FM and CM.

6. Results

First of all, apart from the nested grid experiments, we tested the computational stability and accuracy of this system of equations. With the coarse mesh, time
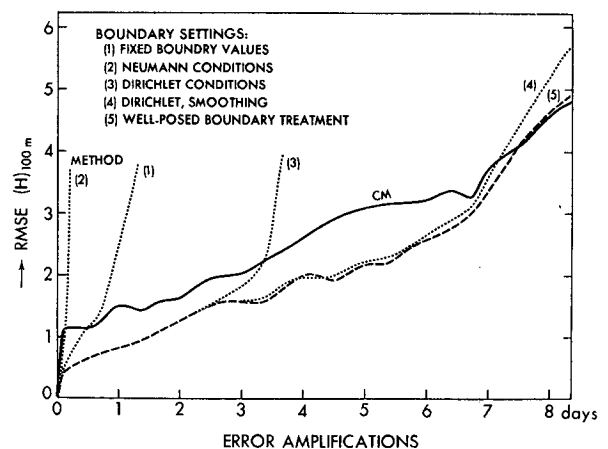

FIG. 4. Evolution of height differences.

[5] We would like to use Set (5) also, but the computing machine is no longer available.

integrations were performed for 30 days both with the explicit, leap-frog scheme ($\Delta t = 5$ min) and with the semi-implicit scheme ($\Delta t = 30$ min). The calculations were stable, and the conservation of kinetic energy and enstrophy turned out to be excellent in both cases. In addition, the two solutions for the explicit and the semi-implicit schemes are quite close to each other as shown in Fig. 3. This is perhaps the most surprising in view of the fact that any two predictions always depart from each other with just a slight difference in the initial conditions—the "predictability decay." In the present calculations, not only the initial conditions but also the governing equations are slightly different in the sense of "explicit" versus "semi-implicit" schemes, yet the two solutions at the 30th day are very similar to each other. This suggests that a careful treatment of the initial condition in the absence of barotropic instability (baroclinic instability in the case of a baroclinic model) can avoid the quick decay of the predictability of solution. Since the success of a nested grid calculation depends on the computational stability of the difference scheme, the test mentioned above is important. The closeness of the two solutions of the explicit and the semi-implicit schemes in CM gives us the confidence that it would be true also in the FM case. Therefore, in the absence of an FM solution of the semi-implicit scheme, we can use an FM solution of the explicit scheme as the reference solution for the semi-implicit scheme. This makes it possible to judge qualitatively the nested grid results.

Let us next turn to the nested grid calculations. It should be pointed out that if the semi-implicit scheme is applied, the solution appears to be relatively smooth. But if the explicit, leap-frog scheme is used, the resultant solution included a large amount of wiggling due

FIG. 5b. Development of height difference in CM. D is the time in Days and I is the index corresponding to the CM but counting from the west boundary of the LFM rather than from the CM area.

to gravity waves, which are presumably caused by the imbalance in the flow field inside as well as at the boundaries. On the other hand, the solution of the Euler-backward scheme is much smoother compared with that of the leap-frog scheme. More important, the accuracy in the Euler-backward scheme appears better than the leap-frog scheme as measured by the rms error, so far as the nested grid calculation is concerned. Hereafter, we will only present the results of the Euler-backward version for the explicit scheme.

The five boundary settings for LFM calculations of the explicit scheme discussed in the previous section were examined. Fig. 4 shows the time evolutions of the root-mean-square difference (or error) of the geopotential height for each of LFM integrations from the reference solution (FM). It is interesting to note that with Boundary Set (1), i.e., the fixed boundary values, computational instability did not occur until the 1.5th day, but with Set (2), i.e., the Neumann conditions, the calculation blew up before the 1st day. Boundary Set (3) is an overspecification. The calculation continued until 3.5th day, then trouble started at the outflow boundary. The integrations with Sets (4) and (5), i.e., LFM-4 and LFM-5, respectively, were most successful and the calculations were still stable up to 8.3th day calculated. To evaluate the advantage of the LFM calculations over the CM calculation, the difference of the CM solution from the FM solution is also displayed. Overall, the LFM's give better results than the CM, in particular, with LFM-4 and LFM-5, the advantage of the nested grid method is significant up to about 6.5th day but disappears after about 7.0th day.

Fig. 5a included the profile in the x direction (I is the grid index) of rms of height difference averaged
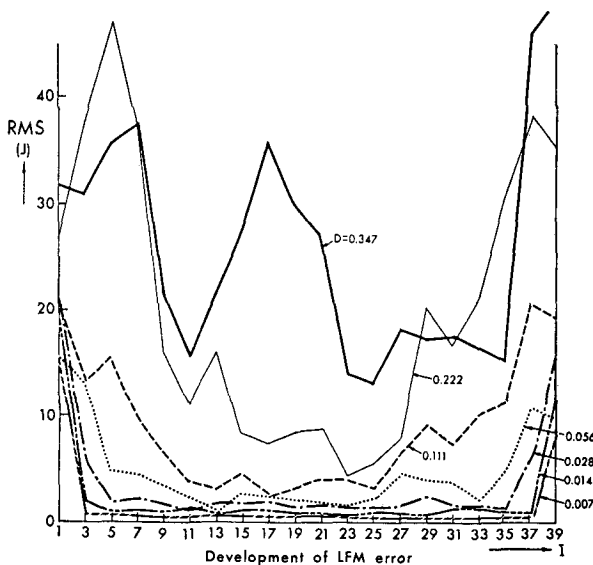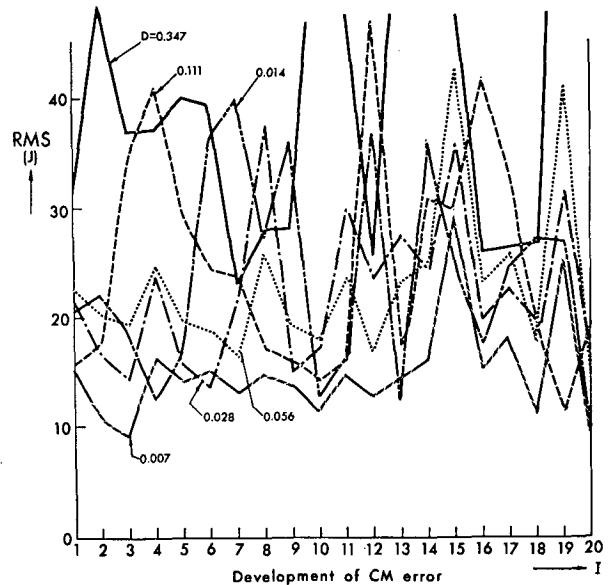

FIG. 5a. Development of height difference in LFM. D is the time in days and I is the index of LFM. Note that every other point of I is skipped for the convenience of comparing with Fig. 5b.
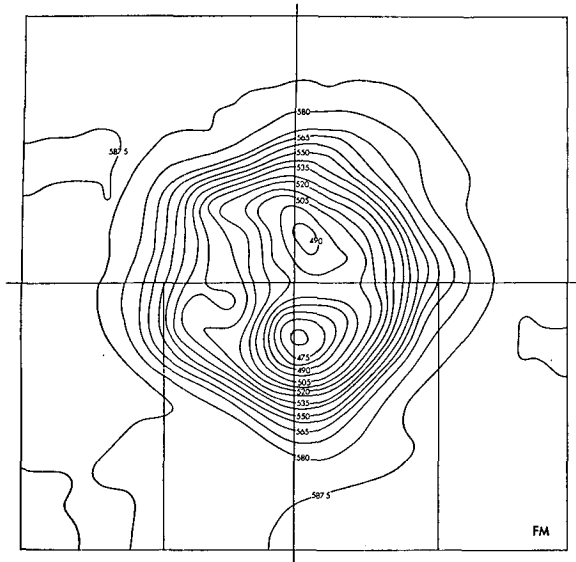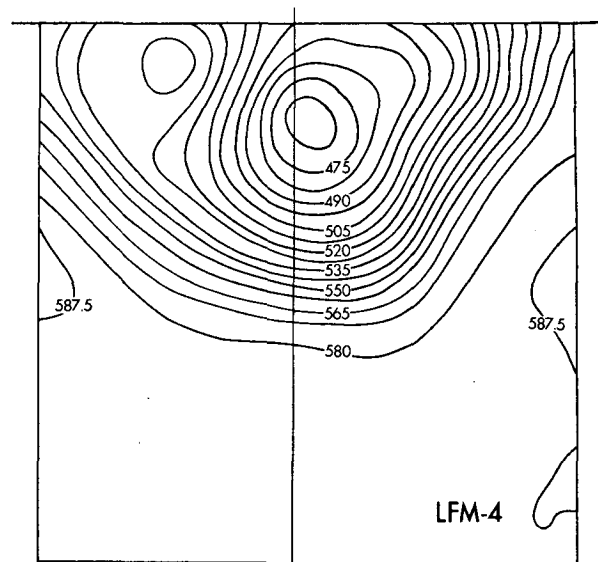
FIG. 6a. FM height field (the reference solution).

FIG. 6c. LFM-4 height field.

over the width of five grids in y-direction, i.e., the 11th through the 15th rows, of LFM-5 case. It is intended to show how the error developed with time and invaded the interior. At the beginning, say during the first $\frac{1}{4}$ day, the error remained near the boundaries, so that the solution in the interior part of the limited domain was very accurate. However, the error amplified and propagated all over the domain as time went on. At the outflow boundary (on the right side of the figure), the growth of error seemed more rapid. Fig. 5b is a similar figure but for the CM. Since the boundary for the CM is far away, the error in the limited region is mainly due to the grid resolutions, not the boundary, so that the

magnitude of the rms difference (error) is distributed equally everywhere and grows at almost the same rate.

To provide a qualitative impression of the nested grid results, the contour lines of geopotential height field are shown in Figs. 6a–6d, where the results are all for the 6.0th day. Fig. 6a is the reference solution (FM), Fig. 6b, the CM, Fig. 6c the LFM-4 and Fig. 6d is the LFM-5. In this particular example of flow pattern, the solutions for both meshes of the large domain are not much different; the only difference is found in the phase speed of waves, the sharpness of the troughs and the amplitude of the system, in particular, the low near the center. Consequently, the effect of the LFM does not look striking in this particular example. Nevertheless,
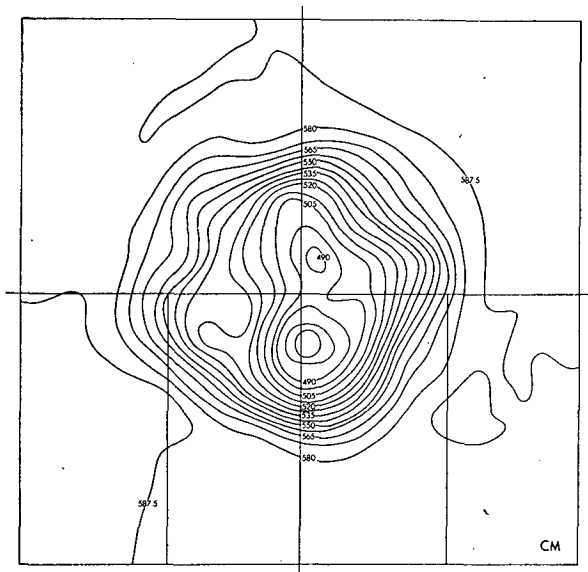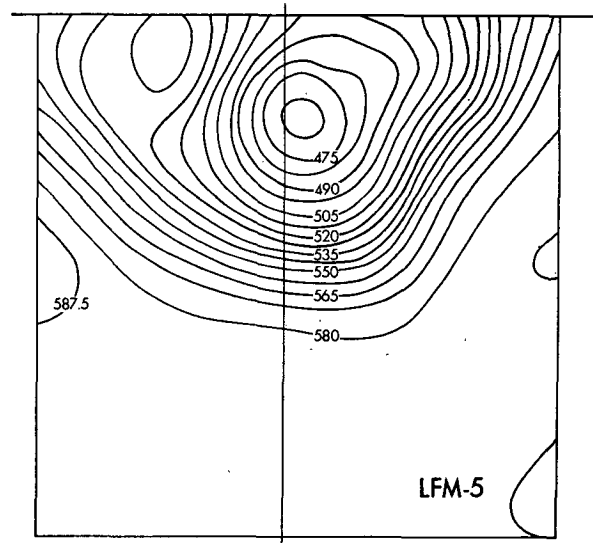
FIG. 6b. CM height field.

FIG. 6d. LFM-5 height field.

the important point is the improved accuracy, especially that of the level of the low, in the LFM over the CM. It is hoped that a greater advantage (in quality, not in the length of time before the nested grid loses its advantage) will be achieved in the baroclinic case.

When the semi-implicit scheme with Boundary Set (4) was applied to the limited area fine mesh grid, it was found that the integration was stable until the 5.2th day. The quality of the solution with this scheme in regard to gravity waves is better than that with the leap-frog method, but is worse than that with the Euler-backward method of the explicit scheme. The semi-implicit scheme has one very attractive merit. The speed of integration is about four times faster than the leap-frog method for the usual problem (i.e., the non-nested grid problem), and is about eight times faster than the Euler-backward method of the explicit scheme. For the nested grid calculation, this advantage is even greater. In the relaxation process of solving the Helmholtz equation in the semi-implicit scheme, the height field obtained in the CM is used as the initial guess, the result is that the speed is increased to about eleven times compared with that of the explicit Euler-backward scheme.

In summary, the following points are concluded. The tests conducted using boundary conditions Sets (4) and (5) gave satisfactory results. Set (5) is a well-posed set of boundary conditions and no empirical treatment was used to avoid computational trouble. However, it is simpler to apply the Set (4) conditions than it is to apply those of Set (5). In this respect, Set (4) may be preferred, especially in connection with a complicated system of equations.

7. Conclusions

A new set of well-posed physical boundary conditions —the specification of the normal velocity component at all boundaries and the tangential component at the inflow boundaries—is proposed for the barotropic primitive equation. In order to apply boundary conditions to a system of finite difference equations, it is often the case that additional boundary conditions should be specified. The present system of finite difference equations is no exception. These additional conditions are provided by extrapolation of the values inside the domain using the upwind method and the pseudo-characteristic method. With this set of numerical boundary conditions, i.e., Set (5), numerical calculations for the nested grid model were carried out successfully. The Dirichlet conditions with local boundary smoothing, i.e., Set (4) proved almost as good as Set (5) in the present experiments where the ratio of grid jump is 2 to 1. The merit of Set (4) is that the boundary setting is extremely simple and that it is not necessary to know the detailed properties of the equations.

These tests revealed that the nested grid model gives solutions that are better than that of the large area

coarse mesh grid up to about 7.0 days and significantly so up to 6.5 days in the explicit, Euler-backward scheme case. In particular, for the first $\frac{1}{4}$ day, the solution in the interior part of the limited domain is very accurate. The semi-implicit scheme is very advantageous in speed for the nested grid model; it is about 11 times faster than the explicit Euler-backward scheme. On the other hand, the leap-frog explicit scheme is twice as fast as the explicit Euler-backward scheme. However, both schemes, the explicit leap-frog and the semi-implicit, are inferior to the explicit Euler-backward scheme in the quality of solution when the nested grid is used.

APPENDIX

Pseudo-characteristic Method

In order to extrapolate the values inside a domain to the boundary, an appropriate characteristic equation is selected and the equation is approximated by a one-sided difference equation. In the problem of a two-dimensional flow, the characteristic, called the Monge cone, consists of a family of characteristic generators which travel in different directions. Therefore, this cone is not suitable for the boundary extrapolation.

To overcome this difficulty we propose here to use the projection of the Monge cone on the $x-t$ or $y-t$ plane, on which the extrapolation is performed. Let us first take the $x-t$ plane, i.e., the extrapolation on the east or the west boundary. For this purpose, we use equations (1A) and (1C). Considering these equations as functions of u and ϕ and treating v and the derivatives in y as parameters, we have virtually "two-dimensional" equations for which characteristics can be obtained. Multiplying (1A) by $\pm a$ and adding the resulting equations to (1C), we have

$$\left(\frac{\partial}{\partial t}+m(u\pm a)\frac{\partial}{\partial x}\right)(\phi\pm au)$$
$$=\pm a(fv-mvu_y)+(\Phi_0+\phi)um_x$$
$$-m\phi u_x-m^2[(\Phi_0+\phi)v/m]_y \quad (P1)$$

where Φ_0 is the mean geopotential and $a\equiv\Phi_0^{\frac{1}{2}}$ is the surface wave speed. Since the equations so obtained are

not really characteristics, we shall call them "pseudo-characteristics." The third term on the right hand side is much smaller than $m\Phi_0 u_x$ or $ma(a \pm u)u_x$ so that it does not have any significant effect on the direction of characteristics. Therefore it is moved to the right hand side. Since we are dealing with large scale motions, a is larger than u, therefore $(u \pm a)$ have both signs. Consequently, one of the characteristics travels upstream and the other downstream. The effect of the domain of dependence in y is kept implicitly in the terms on the right hand side. The upwind or the backward-time scheme (see Chen, 1973) can be used for these pseudo-characteristics, so that the extrapolation of ϕ or u to the east or west boundary is made with these methods.

Similar characteristics on $y-t$ plane can be obtained by using Eqs. (1B) and (1C), considered as functions of v and ϕ in y and t coordinates.

$$\left[\frac{\partial}{\partial t} + m(v \pm a)\frac{\partial}{\partial x} \right](\phi \pm av)$$

$$= \mp a(fu \pm muv_x) + (\Phi_0 + \phi)vm_y$$

$$- m\phi v_y - m^2[(\Phi_0 + \phi)u/m]_x. \quad (P2)$$

The upwind or the backward-time scheme (in $y-t$, rather than $x-t$, coordinates) is used to write one-sided difference equations for obtaining ϕ or u at the north or south boundary.

REFERENCES

Asselin, R., 1972: Integration of a semi-implicit model with time-dependent boundary conditions. *Atmosphere*, **10**, 44–55.

Bengtsson, L., and L. Moen, 1971: An operational system for numerical weather prediction. In *Satellite and Computer Applications to Meteorology*, WMO-No. 283.

Birchfield, G. E., 1960: Numerical prediction of hurricane movement with the use of a fine grid. *J. Meteor.*, **17**, 404–414.

Birkhoff, G., R. S. Varga, and D. Young, 1962: Alternating direction implicit methods. *Advances in Computers*, F. L. Alt, and M. Rubinoff, Eds., New York, Academic Press.

Browning, G., H. Kreiss, and J. Oliger, 1973: Mesh refinement. *Math. Comp.*, **27**, 29–39.

Charney, J. G., 1962: Integration of the primitive and balance equations. *Proc. Int. Sym. Num. Wea. Pred.*, Tokyo, 131–152.

Chen, J. H., 1971: Finite difference methods and the leading edge problem, Ph.D. Thesis, AMS Dept. Princeton University, July.

——, 1973: Numerical boundary conditions and computational modes. *J. Comp. Phys.*, **13**, 522–535.

Davies, C., 1973: On the initial-boundary value problem of some geophysical fluid flows. *J. Comp. Phys.*, **13**, 398–422.

Elvius, T., and A. Sundström, 1973: Computationally efficient schemes and boundary conditions for a fine-mesh barotropic model based on the shallow-water equations. *Tellus*, **25**, 132–156.

Fox, L., 1962: *Numerical Solution of Ordinary and Partial Differential Equations*. London, Pergamon Press.

Garabedian, P. R., 1964: *Partial Differential Equations*. New York, Wiley.

Grammeltvedt, A., 1969: A survey of finite-difference schemes for the primitive equations for a barotropic fluid. *Mon. Wea. Rev.* **97**, 384–404.

Harrison, E. J., Jr., and R. L. Elsberry, 1972: A method for incorporating nested finite grids in the solution of systems of geophysical equations. *J. Atmos. Sci.*, **29**, 1235–1245.

Hill, G. E., 1968: Grid telescoping in numerical weather prediction. *J. Appl. Meteor.*, **7**, 29–38.

Hockney, R. W., 1965: A fast direct solution of Poisson's equation using Fourier analyses. *J. of the Association for Computing Machinery*, **12**, 95–113.

Howcroft, J. G., 1966: Fine-mesh limited-area forecasting model. Tech. Report, 188, U. S. Weather Service, 155 pp.

Jones, R. W., 1973: A nested grid method for a three-dimensional model of a tropical cyclone. Rept. National Hurricane Research Lab., Miami, Fla.

Koss, W., 1971: Numerical integration experiments with variable resolution two-dimensional Cartesian grids using the box method. *Mon. Wea. Rev.*, **99**, 725–738.

Kurihara, Y., 1965: On the use of implicit and iterative methods for the time integration of the wave equation. *Mon. Wea. Rev.*, **93**, 33–46.

Kwizak, M., and A. J. Robert, 1971: A semi-implicit scheme for grid point atmospheric models of the primitive equations. *Mon. Wea. Rev.*, **99**, 32–36.

McPherson, R. D., 1971: Note on the semi-implicit integration of a fine mesh limited-area prediction model on an offset grid. *Mon. Wea. Rev.*, **99**, 242–246.

Mathur, M. B., 1972: Simulation of an asymmetric hurricane with a fine mesh multiple grid primitive equation model. In *NWP over the Tropics*, Dept. of Meteor., Florida State University.

Matsuno, T., 1966: Numerical integrations of the primitive equations by a simulated backward difference method. *J. Met. Soc. Japan*, Ser. 2, **44**, 76–84.

Miyakoda, K., 1960: Test of convergence speed of iterative methods for solving 2 and 3 dimensional Elliptic-type differential equations. *J. Meteor. Soc. Japan*, **38**, 107–124.

Nitta, T., 1962: The outflow boundary condition in numerical time integration of advection equations. *J. Meteor. Soc. Japan*, **40**, 13–24.

Ogura, M., 1969: A direct solution of Poisson's equation by dimension reduction method. *J. Meteor. Soc. Japan*, **47**, 319–323.

Ogura, Y., and J. G. Charney, 1962: A numerical model of thermal convection in the atmosphere. *Proc. Intern. Sym. Num. Wea. Pred.*, Tokyo, 431–451.

Ookochi, Y., 1972: A computational scheme for the nesting fine mesh in the prediction model. *J. Appl. Meteor.*, **9**, 545–553.

Peaceman, D. W., and H. H. Rachford, Jr., 1955: The numerical solution of parabolic and elliptic differential equations. *J. Indus. Appl. Math.*, **3**, 28–41.

Price, G. V., and A. K. MacPherson, 1973: A numerical weather forecasting method using cubic splines on a variable mesh. *J. Appl. Meteor.*, **7**, 1102–1113.

Phillips, N. A., and J. Shukla, 1973: On the strategy of combining coarse and fine grid meshes in numerical weather prediction. *J. Appl. Meteor.*, **12**, 763–770.

Platzman, G. W., 1954: The computational stability of boundary conditions in numerical integration of the vorticity equation. *Archiv. für Meteor. Geophys. Bioklim*, A**7**, 29–40.

Renfrew, D. H., 1971: Private communication.

Robert, A. J., 1969: The integration of a spectral model of the atmosphere by the implicit method. *Proc. of WMO/IUGG Symp. on Num. Wea. Pred.*, Tokyo, Japan, 1968. Japan Met. Agency, Tokyo, March, pp. V11–19.

Shapiro, M. A., and J. J. O'Brien, 1970: Boundary conditions for fine-mesh limited-area forecasts. *J. Appl. Meteor.*, **9**, 345–349.

Wang, H. H., and P. Halpern, 1970: Experiments with a regional fine-mesh limited-area forecasts. *J. Appl. Meteor.*, **9**, 545–553.

Williams, G. P., 1969: Numerical integration of the three-dimensional Navier-Stokes equations for incompressible flow. *J. Fluid Mech.*, **37**, Part 4, 727–750.

Williamson, D. L., 1973: Description of NCAR's fine-mesh limited-area model and the lateral boundary conditions. Presented at Study Conference on the Modelling Aspects of GATE, 24–27 January 1973 at Tallahassee, Fla.